

Magnetoresistance in heavy fermion metals: Comparison to CeB₆.

D. Parihari, N. S. Vidhyadhiraja

*Theoretical Sciences Unit,
Jawaharlal Nehru Centre For Advanced Scientific Research,
Jakkur, Bangalore 560064, India*

(Dated: June 21, 2024)

A theoretical study of magnetic field (h) effects on single-particle spectra and transport quantities of heavy fermion metals in the paramagnetic phase is carried out. We have employed a non-perturbative local moment approach (LMA) to the asymmetric periodic Anderson model within the dynamical mean field framework. The lattice coherence scale ω_L , which is proportional within the LMA to the spin-flip energy scale, and has been shown in earlier studies to be the energy scale at which crossover to single impurity physics occurs, increases monotonically with increasing magnetic field. The many body Kondo resonance in the density of states at the Fermi level splits into two with the splitting being proportional to the field itself. For $h \geq 0$, we demonstrate adiabatic continuity from the strongly interacting case to a corresponding non-interacting limit, thus establishing Fermi liquid behaviour for heavy fermion metals in the presence of magnetic field. In the Kondo lattice regime, the theoretically computed magnetoresistance is found to be negative in the entire temperature range, which may be understood simply by the suppression of spin-flip scattering in the presence of magnetic field. Direct comparison of the theoretical results to the field dependent resistivity measurements in CeB₆ yields good agreement.

PACS numbers:

I. INTRODUCTION

The investigation of lanthanide/actinide based heavy fermion(HF) systems has been a central theme in condensed matter physics both theoretically and experimentally¹. Their behaviour is quite distinct from conventional clean metals, the basic physics being driven by strong spin-flip scattering from essentially localized f -levels, generating the large effective mass. The periodic Anderson model(PAM) forms the general paradigm within which these materials are studied. The minimal model consists of a regular array of sites, each associated with a localized, non-degenerate f -electron core orbital, coupled to a delocalized conduction electron orbital via a local hybridization. Neighboring conduction electron orbitals are connected via a hopping matrix element and electron interactions enter the model via an on-site coulomb repulsion.

The dynamical mean field theory (DMFT)² has proved to be a very powerful framework for studies of lattice models such as the PAM. Within DMFT, which is exact in the limit of infinite dimensions, the self-energy becomes spatially local or momentum independent. As a consequence, lattice models map onto an effective single-impurity model with a self consistently determined host². Among the various methods that exist for solving the the effective single-impurity problem, the local moment approach (LMA)^{3,4,5,6,7}, a non-perturbative many body method, has proved to be extremely successful within DMFT, in describing paramagnetic heavy fermion systems' spectra and transport^{8,9,10}. An extension to finite magnetic fields in the context of the symmetric periodic Anderson model as appropriate for Kondo insulators was carried out recently¹¹. A comparison of theory to experiments on YbB₁₂ for the gap as a function of field yielded

good agreement. In this work, we extend this approach further to encompass magnetic field effects on spectra and transport of heavy fermion metals. Our focus will be on the strong coupling regime, and the issues that we have studied are spectral functions and magnetoresistance. The paper is organized as follows; the model and formalism are presented in section II, followed, in section III by results for the field evolution of single-particle dynamics and d.c transport. In section IV, experimental magnetoresistance of CeB₆ is compared with theory; and finally we conclude with a brief summary.

II. MODEL AND FORMALISM

The Hamiltonian for the PAM in standard notation is given by:

$$\hat{H} = -t \sum_{(i,j),\sigma} c_{i\sigma}^\dagger c_{j\sigma} + \sum_{i\sigma} (\epsilon_f + \frac{U}{2} f_{i-\sigma}^\dagger f_{i-\sigma}) f_{i\sigma}^\dagger f_{i\sigma} + V \sum_{i\sigma} (f_{i\sigma}^\dagger c_{i\sigma} + h.c.) + \sum_{i\sigma} \epsilon_c c_{i\sigma}^\dagger c_{i\sigma} \quad (1)$$

The first term describes the kinetic energy of the noninteracting conduction (c) band due to nearest neighbour hopping t . The second term refers to the f -levels with site energies ϵ_f and on-site repulsion U , while the third term describes the c/f hybridization via the local matrix element V . The final term represents the c -electron orbital energy. In the limit of large dimensions, the hopping needs to be scaled as $t \propto t_*/\sqrt{Z}$, where Z is the lattice coordination number. We consider the hypercubic lattice, for-which the non-interacting density of states is an unbounded Gaussian ($\rho_0(\epsilon) = \exp(-\epsilon^2/t_*^2)/\sqrt{(\pi t_*)}$).

Particle-hole asymmetry in the PAM enters the problem⁷ through an (i) asymmetric conduction band, *i.e.* $\epsilon_c \neq 0$, or (ii) an asymmetric f-level, $\epsilon_f \neq -\frac{U}{2}$. In general, we may quantify the f-level asymmetry by defining $\eta = 1 + \frac{2\epsilon_f}{U}$, such that $\eta = 0$ is equivalent to particle-hole symmetric f-levels. Our primary interest is in the strong coupling Kondo lattice regime: $n_f \rightarrow 1$ but with arbitrary conduction band filling n_c .

Within DMFT, the PAM may be mapped onto an effective self-consistent impurity problem within DMFT. We choose the local moment approach to solve the effective impurity problem arising within DMFT. For details of LMA developed for use within DMFT in the absence of a field, the reader is referred to some of our previous work^{7,8,9,10}. Magnetic field effects in the symmetric PAM as appropriate to Kondo insulators was recently studied by us¹¹. As discussed in that work, the presence of a global magnetic field results in the Zeeman splitting of the bare electronic energy levels as $\epsilon_{\gamma\sigma} = \epsilon_\gamma - \sigma h_\gamma$, for $\gamma = c$ and f electrons. Here $h_\gamma = \frac{1}{2}g_\gamma\mu_B H$ and μ_B is the Bohr magneton; the constants g_f and g_c are the electronic g-factors for the f and c electrons respectively. Although $g_f \neq g_c$ in general, for simplicity we set $g_f = g_c$. The degeneracy of the symmetry broken solutions at the mean-field level (denoted by A and B) is lifted by a magnetic field. We consider here $h > 0$ for which $|\mu(h)|$ (A-type) is the sole solution. The Feenberg self energy^{7,8,11} becomes a functional solely of the A-type Green's function, *i.e.* $S_\sigma(\omega) \equiv S_\sigma[G_{A\sigma}^c]$. Since the B-type solution does not exist, the label 'A' will be implicit in the following.

In presence of a uniform magnetic field, the LMA Green functions are given by

$$G_\sigma^c(\omega, T, h) = \left[\omega^+ + \sigma h - \epsilon_c - S_\sigma^c[G_\sigma^c] - \frac{V^2}{\omega^+ + \sigma h - \epsilon_f - \tilde{\Sigma}_\sigma(\omega, T, h)} \right]^{-1} \quad (2)$$

$$G_\sigma^f(\omega, T, h) = \left[\omega^+ + \sigma h - \epsilon_f - \tilde{\Sigma}_\sigma(\omega, T, h) - \frac{V^2}{\omega^+ + \sigma h - \epsilon_c - S_\sigma^c[G_\sigma^c]} \right]^{-1} \quad (3)$$

with $G^\gamma(\omega) = \frac{1}{2}\sum_\sigma G_\sigma^\gamma(\omega)$. The self energy can be written as a sum of the static and dynamic parts as,

$$\tilde{\Sigma}_\sigma(\omega, T, h) = \frac{U}{2}(\bar{n} - \sigma|\bar{\mu}|(T, h)) + \Sigma_\sigma(\omega, T, h) \quad (4)$$

where $|\bar{\mu}|(T, h)$ is the UHF local moment in presence of magnetic field and temperature. The dynamical self-energy within the LMA is given by^{5,11}

$$\begin{aligned} \Sigma_{-\sigma}(\omega, T, h) &= U^2 \int_{-\infty}^{\infty} \int_{-\infty}^{\infty} d\omega_1 d\omega_2 \chi^{-\sigma\sigma}(\omega_1, T, h) \times \\ &\quad \frac{\mathcal{D}_\sigma(\omega_2, h)}{\omega^+ + \omega_1 - \omega_2} h(\omega_1; \omega_2) \quad (5) \\ h(\omega_1; \omega_2) &= \theta(-\omega_1)[1-f(\omega_2, T)] + \theta(\omega_1)f(\omega_2, T) \end{aligned}$$

where $\chi^{-\sigma\sigma}(\omega, T, h) = \pi^{-1}\text{Im}\Pi^{-\sigma\sigma}(\omega, h)$, $f(\omega) = [\exp^{\beta\omega} + 1]^{-1}$ is the Fermi function and $\theta(\omega)$ is the Heaviside step-function. Here, $\Pi^{-\sigma\sigma}(\omega, T, h)$ denotes the transverse spin polarization propagator which can be expressed as $\Pi^{+-} = {}^0\Pi^{+-}/(1 - U{}^0\Pi^{+-})$ where ${}^0\Pi^{+-}$, the bare p-h bubble, is constructed using the field dependent mean-field spectral densities^{3,9}. The host spectral function is given by $\mathcal{D}_\sigma(\omega, h) = -\frac{1}{\pi}\text{Im}\mathcal{G}_\sigma(\omega, h)$; where the host/medium Green's function \mathcal{G}_σ is given by,

$$\mathcal{G}_\sigma(\omega, T, h) = \left[\omega^+ - e_f + \sigma x + \sigma h - \frac{V^2}{\omega^+ - \epsilon_c + \sigma h - S^c(\omega, T, h)} \right]^{-1} \quad (6)$$

where the parameters $x = U|\mu|/2$ and e_f are determined at $h, T = 0$ by satisfying the symmetry restoration condition

$$\Sigma_\uparrow^R(\omega = 0; e_f, x) - \Sigma_\downarrow^R(\omega = 0; e_f, x) = U|\bar{\mu}(e_f, x)|. \quad (7)$$

and the Luttinger's integral theorem^{7,12}

$$I_L(e_f, x) = \text{Im} \int_{-\infty}^0 \frac{d\omega}{\pi} \frac{\partial \Sigma(\omega)}{\partial \omega} G^f(\omega) = 0 \quad (8)$$

which in turn ensures a Fermi liquid ground state. In practice, it is more convenient numerically to fix x and e_f at the outset and treat U and ϵ_f as unknown parameters to be determined by the above two conditions. As input for the calculation at a given field/temperature, we use the self-energies and Green's functions of a lower field/temperature.

In the limit of infinite dimensions, vertex corrections in the skeleton expansion for the current-current correlation function are absent, hence a knowledge of single-particle dynamics is sufficient within DMFT to determine $\mathbf{q}=0$ transport properties. For $h > 0$, the 3-dimensional isotropic conductivity is computed by adding the contributions from each of the spin channels as

$$\bar{\sigma}(\omega, T, h) = \frac{\sigma_0 t_*^2}{\omega} \sum_\sigma \int_{-\infty}^{\infty} d\omega_1 [f(\omega_1) - f(\omega_1 + \omega)] \times \langle D_\sigma^c(\epsilon; \omega_1) D_\sigma^c(\epsilon; \omega_1 + \omega) \rangle_\epsilon \quad (9)$$

where $\sigma_0 = \frac{\pi e^2}{\hbar a}$ (a is the lattice parameters) and $D_\sigma^c(\epsilon; \omega) = -\frac{1}{\pi}\text{Im}G_\sigma^c(\epsilon; \omega)$. The lattice c -Green's function is given by $G_\sigma^c(\epsilon; \omega) = [\gamma_\sigma(\omega, T, h) - \epsilon]^{-1}$ where $\gamma_\sigma = \omega^+ + \sigma h - \epsilon_c - V^2 \left(\omega^+ + \sigma h - \epsilon_f - \tilde{\Sigma}_\sigma(\omega, T, h) \right)^{-1}$. The ϵ -average is defined by,

$$\langle A(\epsilon; \omega) \rangle_\epsilon = \int_{-\infty}^{\infty} d\epsilon \rho_0(\epsilon) A(\epsilon; \omega) \quad (10)$$

We now proceed to discuss the results obtained by implementing the finite field and finite temperature LMA.

III. RESULTS AND DISCUSSIONS

In this section, we will discuss the single particle dynamics and transport in presence of magnetic field using LMA. Our primary focus is on the strong coupling Kondo lattice regime (where $n_f \rightarrow 1$, but n_c is arbitrary). Before discussing the finite field calculations, we will review a few well established concepts. At $T = 0$ and $h = 0$ ⁷, the strong coupling Kondo lattice regime is characterized by an exponentially small (in strong coupling) low-energy scale $\omega_L = ZV^2/t_*$. The single-particle properties of the asymmetric PAM exhibit scaling in terms of ω/ω_L for a fixed ϵ_c and η . For finite- T and $h = 0$, the spectra $D^c(\omega)$ and $V^2D^f(\omega)$ exhibit scaling in terms of ω/ω_L and T/T_L . We have shown in a recent work on the symmetric PAM ($T = 0$) that such scaling in terms of $\tilde{\omega}_h = \omega/(Z(h)V^2)$ for a fixed effective field (detailed description is in¹¹) holds good in the presence of field as well.

To see if such scaling occurs for the asymmetric case, we carry out a low frequency Fermi liquid analysis of the Green's functions by expanding the self-energy about the Fermi level to first order in ω as,

$$\Sigma_\sigma^R(\omega, h) = \Sigma_\sigma^R(0, h) + (1 - \frac{1}{Z_\sigma(h)})\omega \quad (11)$$

Substituting equation 11 in equations 2 and 3, we find that the spin dependent spectral functions are just renormalized versions of their non-interacting counterparts and are given by (neglecting the 'bare' terms h and ω in the strong coupling limit),

$$D_\sigma^c(\omega; h) \xrightarrow{\omega \rightarrow 0} \rho_0 \left(-\epsilon_c - \frac{1}{\tilde{\omega}_\sigma - \tilde{\epsilon}_f^* + \sigma h_{eff}^\sigma} \right) \quad (12)$$

$$D_\sigma^f(\omega; h) \xrightarrow{\omega \rightarrow 0} \frac{t_*^2}{V^2(\tilde{\omega}_\sigma - \tilde{\epsilon}_f^* + \sigma h_{eff}^\sigma)^2} D_\sigma^c(\omega; h) \quad (13)$$

where $\tilde{\omega}_\sigma = \omega t_*/(Z_\sigma(h)V^2)$ and the renormalized f -level ($\tilde{\epsilon}_f^*$) and h_{eff}^σ can be expressed as,

$$\tilde{\epsilon}_f^* = \frac{t_*}{V^2}(\epsilon_f + \frac{U\bar{n}}{2} - \frac{\sigma U\bar{\mu}}{2} + \Sigma_\sigma^R(0, 0)) \quad (14)$$

and

$$h_{eff}^\sigma = \frac{t_*}{V^2}(h - \sigma(\Sigma_\sigma^R(0, h) - \Sigma_\sigma^R(0, 0))) \quad (15)$$

Using the SR condition, equation 7, it is easy to see that the effective f -level, $\tilde{\epsilon}_f^*$ is spin independent.

From equations 12 and 13, we can infer the following: (i) The spin dependent spectra $D_\sigma^c(\omega, h)$ and $V^2D_\sigma^f(\omega, h)$ should exhibit scaling in terms of $\tilde{\omega}_\sigma$ for a fixed h_{eff}^σ *i.e.*, for a fixed h_{eff}^σ , if we plot the spin dependent spectra *vs* $\tilde{\omega}_\sigma$ for different values of U , they should collapse onto a single curve at the low energy regions for a particular h_{eff}^σ . This is shown in figure 1 where in the insets,

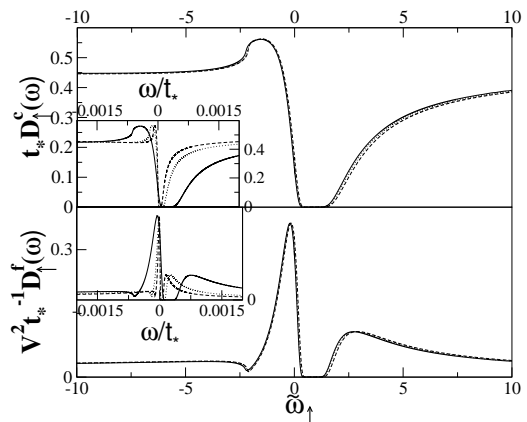


FIG. 1: Insets: LMA spin dependent conduction and f -electron spectra *vs* bare frequency ω/t_* for $\epsilon_c=0.3$, $\eta \rightarrow 0$, $V^2 = 0.2$ and $T = 0$ for three parameter sets: $U \sim 5.1$ and $\tilde{h} = 0.3$ (solid), $U \sim 6.1$ and $\tilde{h} = 0.25$ (dotted), $U \sim 6.6$, and $\tilde{h} = 0.24$ (dashed) for fixed $h_{eff}^\uparrow = 0.39$ (where $\tilde{h} = h/(Z(0)V^2)$). Main: The same spectra when plotted *vs* $\tilde{\omega}_\uparrow = \omega t_*/(Z_\uparrow(h)V^2)$ collapse into one single universal form.

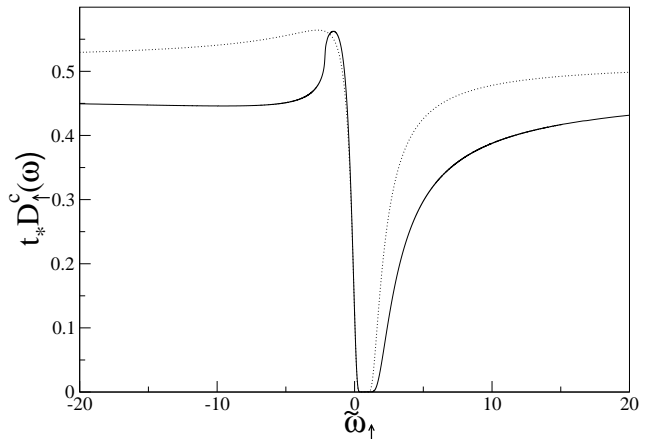


FIG. 2: LMA spin dependent scaling spectra (solid lines) are superposed onto the corresponding non-interacting spectra (dotted lines) for a fixed $h_{eff}^\uparrow = 0.45$ and $\tilde{\epsilon}_f^* = 1.09$.

the conduction electron spectra for up spin (top panel) and the f -electron spectra for up spin (bottom panel) are plotted as a function of the bare frequency ω/t_* with $\epsilon_c=0.3$, $\eta \rightarrow 0$, $V^2 = 0.2$ and $T=0$ for three parameter sets: $U \sim 5.1$ and $\tilde{h} = 0.3$ (solid), $U \sim 6.1$ and $\tilde{h} = 0.25$ (dotted), $U \sim 6.6$, and $\tilde{h} = 0.24$ (dashed) such that $h_{eff}^\uparrow=0.39$ is fixed (where $\tilde{h} = h/(Z(0)V^2)$). In the main panel the same spectra are plotted as a function of $\tilde{\omega}_{h\uparrow}$. We see that when we plot the spectra *vs* bare frequency, they appear very different, but when plotted *vs* $\tilde{\omega}_\uparrow$ (main panel: top and bottom), they collapse onto a single universal form. We have checked that similar universality holds for the down spin also for a fixed h_{eff}^\downarrow .

(ii) The spin dependent conduction and f -electron spectra

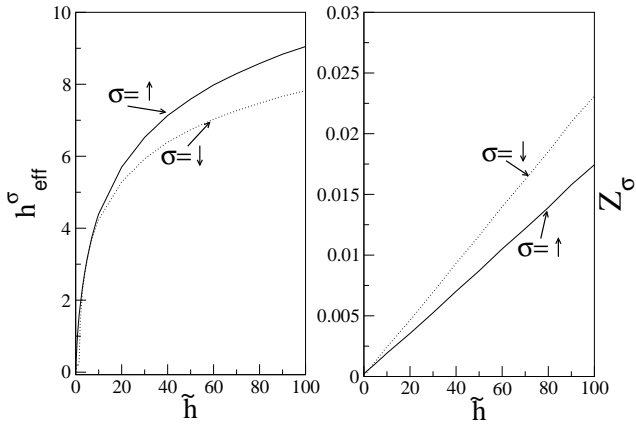


FIG. 3: Left panel: h_{eff}^{σ} vs $\tilde{h} = h/(ZV^2)$ (Z is the quasiparticle weight for $h = 0$) for $\epsilon_c = 0.3$, $\eta \rightarrow 0$, $T = 0$ and $U = 6.6$. Right panel: Spin dependent quasiparticle weight $Z_{\sigma}(h)$ vs $\tilde{h} = h/(Z_{\sigma}V^2)$ for the same parameters.

$D_{\sigma}^c(\omega)$ and $V^2 D_{\sigma}^f(\omega)$ should adiabatically connect to the non-interacting limit at low energy scales *i.e.*, if we take the c -electron and f -electron fields as zero and h_{eff}^{σ} respectively, substitute for ϵ_f the renormalized f -level ($\tilde{\epsilon}_f^*$) and compute the spectra in the non-interacting limit; then the interacting spectra and the non-interacting spectra should be same at low energy scales. This is shown in figure 2, where the spin dependent scaling spectra $D_{\uparrow}^c(\omega)$ for the interacting case ($U = 6.6$) is superposed onto the non-interacting spectra. We see from figure 2 that both the curves are almost identical near the Fermi level. This demonstrates adiabatic continuity of the strong coupling regime to the non interacting limit which represents Fermi liquid behaviour in presence of magnetic field for the asymmetric case (in parallel to the symmetric PAM¹¹).

To see the effect of magnetic field on the spin dependent effective fields h_{eff}^{σ} and the spin dependent quasiparticle weights Z_{σ} , we have plotted in figure 3, the spin dependent effective fields ($h_{\text{eff}}^{\uparrow}$ and $h_{\text{eff}}^{\downarrow}$) vs \tilde{h} (left panel) and the spin dependent quasiparticle weights ($Z_{\uparrow}(h)$ and $Z_{\downarrow}(h)$) vs \tilde{h} (right panel). We see that $Z_{\uparrow}(h) \cong Z_{\downarrow}(h)$ and $h_{\text{eff}}^{\uparrow} \cong h_{\text{eff}}^{\downarrow}$ up to about $\tilde{h} \sim 10.0$. So, we can assume that the spin summed spectra $D^c(\omega)$ and $V^2 D^f(\omega)$ also should exhibit scaling in terms of $\tilde{\omega}_{\sigma}$ for low fields (up to $\tilde{h} \sim 10$) for a fixed h_{eff}^{σ} . To see this, we plot up spin scaling spectra (main panel) as well as corresponding spin summed spectra in figure 4 (insets) for $U = 5.1$ (solid line) and $U = 6.6$ (dotted line) for a fixed $h_{\text{eff}}^{\uparrow} = 4.2$ ($\tilde{h} \sim 10.0$) and $T = 0$. Indeed, we see that the spin summed spectra also exhibit universal scaling and adiabatic continuity at low energy scales.

Now we turn to the LMA results for the field evolution of the asymmetric PAM for a fixed temperature. In figure 5, we show $T = 0$ spin summed conduction and f -electron scaling spectra for various fields: $\tilde{h} = 0$ (solid), 0.5 (dotted), 1.0 (dashed), 1.5 (dot-dashed), 2.0 (bold solid), 3.0 (bold dotted), 5.0 (bold dashed) and 10.0 (bold dot-dashed)

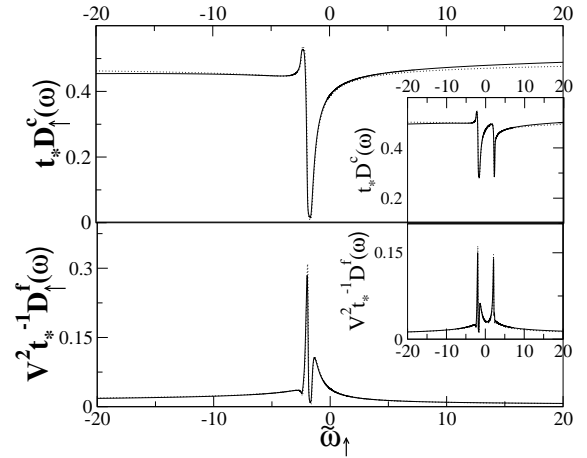


FIG. 4: Main panel: LMA up-spin conduction electron scaling spectra (top) and up spin f -electron scaling spectra (bottom) vs $\tilde{\omega}_{h\uparrow}$ for $\epsilon_c = 0.3$, $\eta \rightarrow 0$ and $V^2 = 0.2$ for two parameter sets: $U \sim 5.1$ and $\tilde{h} = 10.0$ (solid), $U \sim 6.6$ and $\tilde{h} = 9.0$ (dotted) for fixed $h_{\text{eff}}^{\uparrow} = 4.2$. Insets: The corresponding spin summed conduction and (top) f -electron (bottom) scaling spectra vs $\tilde{\omega}_{h\uparrow}$ for the same parameter sets. Spin summed as well as the spin dependent spectra exhibit universality/scaling in the strong coupling regime.

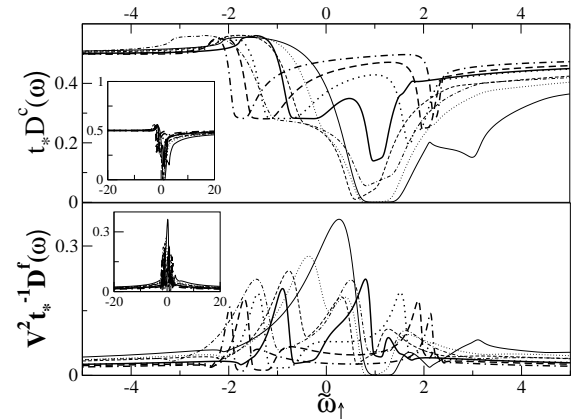


FIG. 5: LMA conduction and f -electron spectra vs $\tilde{\omega}_{h\uparrow} = \omega/(Z_{\uparrow}(h)V^2)$ for $U = 6.6$, $\epsilon_c = 0.3$ and $\eta \rightarrow 0.0$ for $\tilde{h} = 0$ (solid), 0.5 (dotted), 1.0 (dashed), 1.5 (dot-dashed), 2.0 (bold solid), 3.0 (bold dotted), 5.0 (bold dashed) and 10.0 (bold dot-dashed) for $T = 0$.

(bold solid), 3.0 (bold dotted), 5.0 (bold dashed) and 10.0 (bold dot-dashed) and fixed interaction strength $U = 6.6$. In our earlier work on the symmetric PAM¹¹, we have shown that there is a gap at the Fermi level, as there must be for a Kondo insulator. But in the asymmetric limit $\epsilon_c = 0.3$, $h = 0$ (see figure 5), the gap moves away from the Fermi level and becomes a pseudo-gap. The width of the Kondo resonance at the Fermi level is proportional to the low-energy scale $\omega_{L\sigma} = Z_{\sigma}(0)V^2$. The insets of the the figure 5 show the spectra on a large frequency scale. It is seen that for very large frequencies

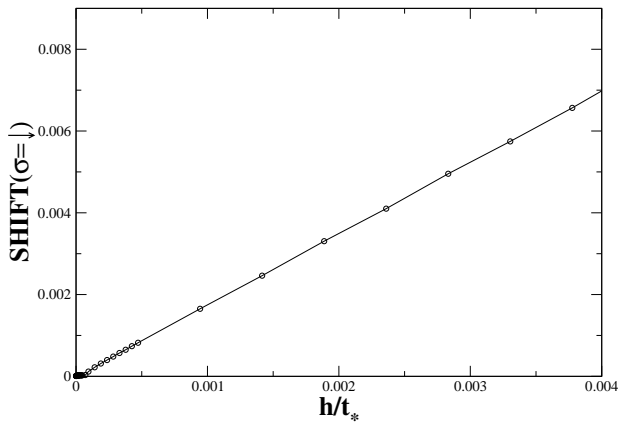


FIG. 6: Shift of down bands *vs* field for $U = 6.6$: the down bands do shift linearly with the field.

the tails of the spectra for all fields are identical which is physically natural since one can expect that the effect of the field should dominate only for $|\tilde{\omega}_\sigma| \lesssim h/(Z_\sigma(h)V^2)$. Now with increasing magnetic field, the lattice Kondo resonance splits into two peaks, with the distance between the peaks also increasing. Qualitatively we can understand the results as follows: In the non-interacting limit for the symmetric case, we have shown that the c and f -levels shift rigidly due to the Zeeman effect. The same concept is valid for the asymmetric case also for the non-interacting limit *i.e.* the spectral function for the up and down spin bands shift rigidly away from the Fermi level. In the presence of interactions, in parallel to the symmetric case, the shift of the spin bands should not be rigid due to the competition between Zeeman splitting and Kondo screening. And indeed, we find that the distance between the two peaks is not $2\hbar$; however the up and down bands do shift linearly with field away from the Fermi level (see figure 6) in the strong coupling regime.

Now, we turn our attention to field-dependent transport properties. At finite temperature, as the spin summed conduction electron spectra exhibits universal scaling in terms of $T/(Z_\sigma(h)V^2)$ in the strong coupling regime for low fields, we expect that the resistivity will also exhibit scaling in terms of $T/(Z_\sigma(h)V^2)$. The classic HF metallic resistivity increases with temperatures (initially as T^2), goes through a maximum T_{max} (the peak position of $\rho(T)$) and then decreases with temperature characteristic of single impurity behaviour. We observe the same form for the resistivity in our calculations. In figure 7 (top), the resistivity *vs* scaled temperature $T/\omega_{L\sigma}$ is shown for both $\sigma = \uparrow, \downarrow$ and for a range of fields: $\tilde{h} = 0.0$ (solid), 0.06 (dotted), 0.5 (dashed), 0.5 (long-dashed) and 2.0 (dot-dashed) with U equal to 6.6 . Negative magnetoresistance is observed over the entire range of temperatures as shown in figure 7 (bottom). Suppression of the spin-flip scattering is the underlying reason for the reduction in resistivity in the presence of a field. At higher temperatures, the effect of magnetic field is small compared to the temperatures. So, the magne-

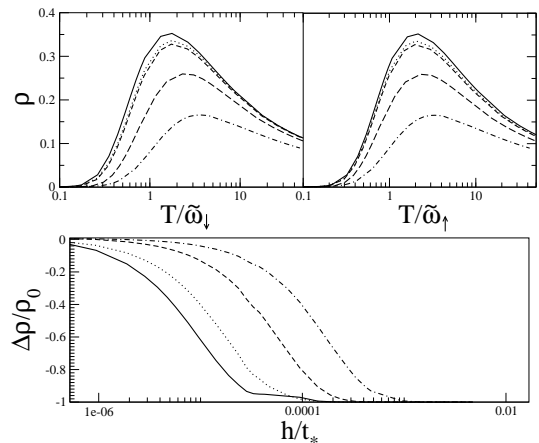


FIG. 7: Top: Left panel: Resistivity *vs* $\tilde{\omega}_{h\downarrow}$ for the same parameters, but for the various fields ($\tilde{h} = 0.0$ (solid), 0.06 (dotted), 0.1 (dashed), 0.5 (long dashed) and 2.0 (dot-dashed). Right panel: Resistivity *vs* $\tilde{\omega}_{h\uparrow}$ for the same sets of parameters. Bottom: Magnetoresistivity *vs* bare fields h/t_* for $U = 6.6$, $\epsilon_c = 0.3$ and $\eta \rightarrow 0.0$ for $\tilde{T} = 0.3$ (solid), 0.6 (dotted), 2.0 (dashed), 6.0 (dot-dashed).

toresistance is almost zero. Next, we compare our theoretical results with experiment.

IV. COMPARISON TO CeB_6

In this section we want to compare our theoretical results with experiment on CeB_6 . The magnetoresistance of CeB_6 crystal has been measured in the temperature range from 3 to $300K$ up to magnetic field 85 KOe by Takase et. al.¹³. From an earlier study¹⁰, it is known that the HF system CeB_6 , belongs to the moderately strong coupling regime. Hence we have taken the theoretical results to compare with experiments on CeB_6 for the following parameters: $U=2.4$, $\epsilon_c=0.5$, $\eta \rightarrow 0$ and $V^2 = 0.2$. To compare the experimental results with our theory, two fundamental requirements need to be met. First requirement is that, we should extract the contribution to the measured resistivity from phonons ($\rho_{ph}(T)$) and the residual resistivity ($\rho(0)$). This is given by, $\rho_{mag}^{exp}(T) = a(\rho(T) - \rho(0)) - \rho_{ph}(T)$ where, a is a constant which comes from the error of the sample geometry to the measured resistivity. A detailed discussion of this point is given in ref¹⁰. In this work, we simply assume $a = 1$. The second is, the value of low-energy scale is needed for comparing our theoretical results with experiment. For this, we superposed the theoretical resistivity $\rho_{mag}(T)$ onto $\rho_{mag}^{exp}(T)$ for $h = 0$ to calculate the value of the low-energy scale. The value of the low energy scale turns out to be $\omega_L = 2.2K$. Assuming the g -factor to be roughly unity, the magnetic field of $1kOe$ can be translated into multiples of the low energy scale. For $H = 1kOe$, $g\mu_B H \simeq 0.067K \simeq 0.03\omega_L$. Thus the magnetic fields employed in the experiments¹³ turn out

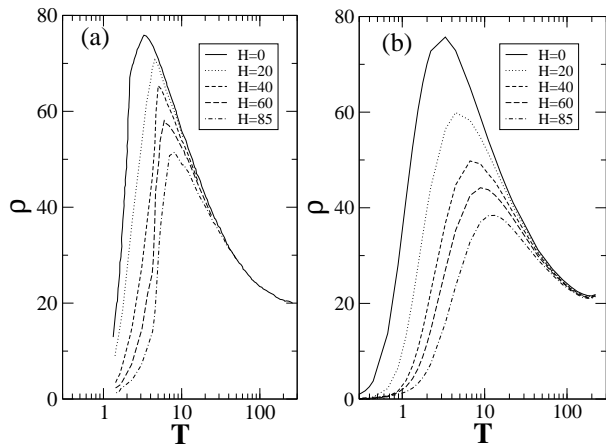


FIG. 8: Resistivity vs temperature of CeB_6 (a) experiment (b) theory for the various fields: $H = 0$ kOe (solid), 20 kOe (dotted), 40 kOe (dashed), 60 kOe (long dashed) and 85 kOe (dot dashed).

to be (in multiples of ω_L), $\tilde{h} = 0, 0.6, 1.2, 1.8$ and 2.5 corresponding to fields of $H = 0, 20\text{kOe}, 40\text{kOe}, 60\text{kOe}$ and 85kOe respectively.

By scaling the theoretical resistivities on the x-axis by the low energy scale and the y-axis by a single multiplicative factor (same for all fields), we show the theoretical computed dc resistivities for the same magnetic fields as the experiment in figure 8 (left). When compared with the experimental results in figure 8 (right), good qualitative agreement is found.

V. CONCLUSIONS

To summarise, we have employed a non-perturbative local moment approach to the asymmetric periodic Anderson model within DMFT in presence of magnetic field. Field-dependent dynamics and transport properties of the model have been computed. In the strong coupling Kondo lattice regime of the model, the local c - and f -electron spectral functions are found to exhibit universal scaling, being functions solely of $\omega/\omega_{L\sigma}, T/\omega_{L\sigma}$ ($\omega_{L\sigma}$ being the low-energy scale) for a given effective field h_{eff}^σ . Although the externally applied field is globally uniform, the effective local field experienced by the c - and f -electrons differs because of correlation effects. Fermi liquid behaviour has been established even in presence of magnetic fields through adiabatic continuity to the non-interacting limit. In presence of magnetic field, the quasi-particle peak at $h = 0$ and $T = 0$ splits into two. The shift of these peaks away from the Fermi level is not rigid due to the competition between local moment screening and Zeeman spin-polarization. Although these shifts vary linearly with the field in strong coupling, the slope is not the same as the non-interacting limit. Finally, a comparison of theoretical magnetoresistance results with experiment yields good agreement.

Acknowledgments

We would like to thank Prof. David Logan for extremely fruitful discussions, and Department of Science and technology, India for funding.

- ¹ N. Grewe and F. Steglich, *Handbook on the Physics and Chemistry of Rare Earths*, edited by K. A. Gschneider, Jr. and L. Eyring (Elsevier, Amsterdam, 1991), Vol. 14; A. C. Hewson, *The Kondo problem to Heavy Fermions*, (Cambridge University Press, 1993); G. R. Stewart, *Rev. Mod. Phys.* **73**, 797 (2001).
- ² D. Vollhardt, *Correlated Electron Systems*, edited by V. J. Emery (World Scientific, Singapore, 1993) Vol. 9; T. Pruschke, M. Jarrell and J. K. Freericks, *Adv. Phys.* **44**, 187 (1995); A. Georges, G. Kotliar, W. Krauth and M. Rozenberg, *Rev. Mod. Phys.* **68**, 13 (1996); F. Gebhard, *The Mott Metal-Insulator Transition* (Springer Tracts in Modern Physics **137** Springer, Berlin, 1997).
- ³ D. E. Logan, M. P. Eastwood and M. A. Tusch, *J. Phys.: Condens. Matter* **10**, 2673 (1998).
- ⁴ M. T. Glossop and D. E. Logan, *J. Phys.: Condens. Matter* **14**, 673 (2002); N. L. Dickens and D. E. Logan, *J. Phys.: Condens. Matter* **13**, 4505 (2001).
- ⁵ D. E. Logan and N. L. Dickens, *J. Phys.: Condens. Matter* **14**, 3605 (2002).
- ⁶ D. E. Logan and N. L. Dickens, *Europhys. Lett.* **54**, 227 (2001); D. E. Logan and N. L. Dickens, *J. Phys.: Condens. Matter* **13**, 9713 (2001); D. E. Logan and M. T. Glossop,

- J. Phys.: Condens. Matter* **12**, 985 (2000); M. T. Glossop and D. E. Logan, *J. Phys.: Condens. Matter* **15**, 7519 (2003); M. T. Glossop and D. E. Logan, *Europhys. Lett.* **61**, 810 (2003); R. Bulla, M. T. Glossop, D. E. Logan and T. Pruschke *J. Phys.: Condens. Matter* **12**, 4899 (2000); V. E. Smith, D. E. Logan and H. R. Krishnamurthy, *Eur. Phys. J. B* **32**, 49 (2003)
- ⁷ N. S. Vidhyadhiraja and D. E. Logan, *Eur. Phys. J. B* **39**, 313-334 (2004).
- ⁸ N. S. Vidhyadhiraja, V. E. Smith, D. E. Logan and H. R. Krishnamurthy, *J. Phys.: Condens. Matter* **15**, 4045 (2003).
- ⁹ D. E. Logan and N. S. Vidhyadhiraja, *J. Phys.: Condens. Matter* **17** 2935 (2005).
- ¹⁰ N. S. Vidhyadhiraja and D. E. Logan, *J. Phys.: Condens. Matter* **17** 2959 (2005).
- ¹¹ D. Parihari, N. S. Vidhyadhiraja and D. E. Logan, *Phys. Rev. B* **78**, 035128 (2008).
- ¹² J. M. Luttinger and J. C. Ward, *Phys. Rev.* **118**, 1417 (1960).
- ¹³ A. Takase, K. Kojima, T. Komatsubara and T. Kasuya, *Sol. St. Comm.*, **36** 461 (1980).